Calculation of anharmonic phonon couplings in C, Si, and Ge

David Vanderbilt
Lyman Laboratory of Physics, Harvard University, Cambridge, Massachusetts 02138

Steven G. Louie and Marvin L. Cohen
Department of Physics, University of California, Berkeley, California 94720
and Materials and Molecular Research Division, Lawrence Berkeley Laboratory, Berkeley, California 94720
(Received 20 September 1985)

Frozen-phonon total-energy calculations are used to extract anharmonic phonon couplings for the tetrahedral elements C, Si, and Ge. The local-density approximation is employed, with a localized-orbital basis used for C and a plane-wave expansion used for Si and Ge. The bare interactions between optical phonons are completely determined through fourth order at the Brillouin-zone center. These are used to compute renormalized couplings, in which a vertex is screened by virtual phonons. The renormalized couplings are found to have the *wrong sign* to allow formation of a proposed two-phonon bound state in diamond.

I. INTRODUCTION

The application of the frozen-phonon total-energy approach has emerged as a powerful tool for the calculation of phonon frequencies.[1-3] In this approach, the total energy is calculated self-consistently within the local-density approximation[4] for a series of frozen-phonon geometries, in which the displacements of the atoms correspond to a single normal mode of interest. The dependence of total energy on normal-mode amplitude is calculated, and the spring constant and phonon frequency are obtained from the second derivative of the energy curve.

It has not been widely appreciated that the same approach can be used to extract third[1,2,5] and higher derivatives of the energy vs amplitude curve, and hence to obtain anharmonic coupling constants in the phonon Hamiltonian. Here, we report the first systematic calculation of this kind, in which we determine a set of third- and fourth-order anharmonic coupling constants for optical phonons in C, Si, and Ge. The calculations are carried out using a localized-orbital approach[6,7] for C and a plane-wave expansion[8] for Si and Ge. The results for C have previously appeared in abbreviated form.[9]

Information on such anharmonic terms in the phonon Hamiltonian is of interest for at least two reasons. First, they determine the amplitudes for phonon-phonon interactions. For example, phonon-phonon scattering cross sections and phonon decay lifetimes are determined by the anharmonic couplings. Second, the anharmonic terms are useful constraints upon attempts to develop classical models of the elastic energies in solids. Attempts have previously been made[10,11] to develop force-field models which go beyond the harmonic approximation. It is hoped that such models would give more accurate estimates of the strain energies when bonds are stretched or bent severely enough to exceed the range of applicability of the harmonic approximation. However, the previous models have suffered from the lack of reliable input on the values of these anharmonic terms.

In principle, anharmonic couplings connecting phonons throughout the Brillouin zone could be calculated using supercell techniques. In the present work, however, we have concentrated on the anharmonic couplings for optical phonons at the Brillouin zone center. To date, no reliable experimental or theoretical information has been available on these optical anharmonic terms. Measurements of anharmonic elastic moduli, thermal expansion and thermal conductivity, phonon linewidths, and pressure or stress dependencies of phonon frequencies (Grüneisen parameters) can only give information about purely acoustical or mixed acoustical-optical interactions. Theoretically, empirical force-field models of the Born or Keating type are inadequate, since there is little reason to expect their range of validity to extend beyond the harmonic approximation.

These zone-center optical anharmonic terms are of particular interest in relation to a controversial proposal made some years ago by Cohen and Ruvalds.[12] They pointed out that a sufficiently strong positive fourth-order coupling could cause a pair of optical phonons in the vicinity of the zone center to bind to one another. Such a two-phonon bound state, it was suggested, might explain an anomalous peak in the two-phonon Raman spectrum of diamond.[13] Alternative explanations have been proposed,[14] and the bound-phonon model has remained controversial. The calculations presented here demonstrate that the phonon coupling is actually *negative,* in which case the two-phonon bound state cannot form in diamond.[9]

The plan of the paper is as follows. In Sec. II, we review the derivation and quantization of the phonon Hamiltonian, identify all the anharmonic couplings allowed by symmetry through fourth order, and establish the connection between these couplings and the derivatives of the energy-vs-amplitude curves for frozen phonons along the principle symmetry directions. Section III contains a discussion of the method of the total energy calculations, and a presentation of the results for the anharmonic couplings.

In Sec. IV, these bare couplings serve as the basis for a many-phonon perturbation-theoretic treatment in which the couplings are renormalized by the inclusion of processes involving the exchange of virtual phonons. A screened two-phonon scattering amplitude and an approximate screened phonon frequency are obtained. Finally, we present a summary of the work in Sec. V.

II. PHONON HAMILTONIAN

The phonon Hamiltonian of a crystal may be expanded as[15]

$$H = E_0 + T + V_2 + V_3 + V_4 + \cdots , \tag{1}$$

where

$$V_2 = \frac{1}{2!} \sum_{\substack{\mathbf{mn} \\ ij}} \Phi_{ij}^{\mathbf{mn}} x_i^{\mathbf{m}} x_j^{\mathbf{n}} ,$$

$$V_3 = \frac{1}{3!} \sum_{\substack{\mathbf{mnp} \\ ij}} \Phi_{ijk}^{\mathbf{mnp}} x_i^{\mathbf{m}} x_j^{\mathbf{n}} x_k^{\mathbf{p}} , \tag{2}$$

$$V_4 = \frac{1}{4!} \sum_{\substack{\mathbf{mnpq} \\ ijkl}} \Phi_{ijkl}^{\mathbf{mnpq}} x_i^{\mathbf{m}} x_j^{\mathbf{n}} x_k^{\mathbf{p}} x_l^{\mathbf{q}} .$$

The $ijkl$ are composite indices labeling both the atom in the cell and the Cartesian direction of displacement, and **mnpq** are real-space lattice vectors.

We now specialize to the diamond crystal structure, choosing periodic boundary conditions on a volume containing N cells and $2N$ atoms. The solutions of the secular equation

$$\sum_{\mathbf{nj}} \Phi_{ij}^{\mathbf{mn}} Q_{j;\lambda}^{\mathbf{n};\mathbf{k}} = M\omega_{\mathbf{k}\lambda}^2 Q_{i;\lambda}^{\mathbf{m};\mathbf{k}} \tag{3}$$

are labeled by discrete wave vector $\mathbf{k}$ and a band and polarization index λ. The eigenvectors Q are related to the polarization vectors e by

$$Q_{i;\lambda}^{\mathbf{m};\mathbf{k}} = \frac{1}{\sqrt{2N}} e_{i;\lambda}^{\mathbf{k}} \exp(i\mathbf{k}\cdot\mathbf{m}) . \tag{4}$$

The normal mode coordinates $a_{\mathbf{k}\lambda}$ are defined by

$$x_i^{\mathbf{m}} = \sum_{\mathbf{k}\lambda} Q_{i;\lambda}^{\mathbf{m};\mathbf{k}} a_{\mathbf{k}\lambda} . \tag{5}$$

The elastic energy may be rewritten in terms of the normal mode coordinates as

$$V_2 = \frac{1}{2!} \sum_{\substack{\mathbf{kk}' \\ \lambda\lambda'}} \Phi_{\lambda\lambda'}^{\mathbf{kk}'} a_{\mathbf{k}\lambda} a_{\mathbf{k}'\lambda'} , \tag{6a}$$

$$V_3 = \frac{1}{3!} \frac{1}{\sqrt{2N}} \sum_{\substack{\mathbf{kk'k''} \\ \lambda\lambda'\lambda''}} \Phi_{\lambda\lambda'\lambda''}^{\mathbf{kk'k''}} a_{\mathbf{k}\lambda} a_{\mathbf{k}'\lambda'} a_{\mathbf{k}''\lambda''} , \tag{6b}$$

$$V_4 = \frac{1}{4!} \frac{1}{2N} \sum_{\substack{\mathbf{kk'k''k'''} \\ \lambda\lambda'\lambda''\lambda'''}} \Phi_{\lambda\lambda'\lambda''\lambda'''}^{\mathbf{kk'k''k'''}} a_{\mathbf{k}\lambda} a_{\mathbf{k}'\lambda'} a_{\mathbf{k}''\lambda''} a_{\mathbf{k}'''\lambda'''} , \tag{6c}$$

where

$$\Phi_{\lambda\lambda'}^{\mathbf{kk}'} = \frac{1}{2N} \sum_{\substack{\mathbf{mn} \\ ij}} \Phi_{ij}^{\mathbf{mn}} e_{i;\lambda}^{\mathbf{k}} e_{j;\lambda'}^{\mathbf{k}'} \exp[i(\mathbf{k}\cdot\mathbf{m} + \mathbf{k}'\cdot\mathbf{n})] ,$$

$$\Phi_{\lambda\lambda'\lambda''}^{\mathbf{kk'k''}} = \frac{1}{2N} \sum_{\substack{\mathbf{mnp} \\ ijk}} \Phi_{ijk}^{\mathbf{mnp}} e_{i;\lambda}^{\mathbf{k}} e_{j;\lambda'}^{\mathbf{k}'} e_{k;\lambda}^{\mathbf{k}''} \times \exp[i(\mathbf{k}\cdot\mathbf{m} + \mathbf{k}'\cdot\mathbf{n} + \mathbf{k}''\cdot\mathbf{p})] , \tag{7}$$

$$\Phi_{\lambda\lambda'\lambda''\lambda'''}^{\mathbf{kk'k''k'''}} = \frac{1}{2N} \sum_{\substack{\mathbf{mnpq} \\ ijkl}} \Phi_{ijkl}^{\mathbf{mnpq}} e_{i;\lambda}^{\mathbf{k}} e_{j;\lambda'}^{\mathbf{k}'} e_{k;\lambda''}^{\mathbf{k}''} e_{l;\lambda'''}^{\mathbf{k}'''} \times \exp[i(\mathbf{k}\cdot\mathbf{m} + \mathbf{k}'\cdot\mathbf{n} + \mathbf{k}''\cdot\mathbf{p} + \mathbf{k}'''\cdot\mathbf{q})] .$$

Making use of Eqs. (3) and (4) and orthogonality relations, the harmonic constant can be rewritten

$$\Phi_{\lambda\lambda'}^{\mathbf{kk}'} = \delta_{\lambda\lambda'} \delta_{\mathbf{k},-\mathbf{k}'} M\omega_{\mathbf{k}\lambda}^2 \tag{8}$$

and the harmonic part of the Hamiltonian becomes

$$H_2 = T + V_2 = \tfrac{1}{2} M \sum_{\mathbf{k}\lambda} (\dot{a}_{\mathbf{k}\lambda}^* \dot{a}_{\mathbf{k}\lambda} + a_{\mathbf{k}\lambda}^* a_{\mathbf{k}\lambda} \omega_{\mathbf{k}\lambda}^2) . \tag{9}$$

So far, the analysis has been entirely classical. The normal mode coordinates may now be quantized as

$$a_{\mathbf{k}\lambda} = \left(\frac{\hbar}{2M\omega_{\mathbf{k}\lambda}} \right)^{1/2} (b_{\mathbf{k}\lambda} + b_{-\mathbf{k}\lambda}^\dagger) , \tag{10a}$$

$$\dot{a}_{\mathbf{k}\lambda} = -i\omega_{\mathbf{k}\lambda} \left(\frac{\hbar}{2M\omega_{\mathbf{k}\lambda}} \right)^{1/2} (b_{\mathbf{k}\lambda} - b_{-\mathbf{k}\lambda}^\dagger) . \tag{10b}$$

The phonon creation and annihilation operators $b^\dagger$ and b so defined have the usual boson commutation relations. Equation (9) becomes

$$H_2 = \sum_{\mathbf{k}\lambda} \hbar\omega_{\mathbf{k}\lambda} (b_{\mathbf{k}\lambda}^\dagger b_{\mathbf{k}\lambda} + \tfrac{1}{2}) . \tag{11}$$

The bare phonon self-energy is $\hbar\omega_{\mathbf{k}\lambda}$. The anharmonic terms V_3 and V_4 can be expanded in the creation and annihilation operators by inserting (10a) in (6), determining the bare three-phonon and four-phonon interaction amplitudes.

As we shall see in Sec. IV, the physical phonon self-energies and phonon-phonon scattering amplitudes correspond not to these bare quantities, but rather to screened couplings which are renormalized by the inclusion of virtual phonon processes. If the bare couplings are known, the screened couplings can be calculated from many-body phonon perturbation theory. This will be illustrated in Sec. IV.

Ideally, one could proceed as follows. First, the bare harmonic and anharmonic elastic constants $\Phi_{\lambda\lambda'}^{\mathbf{kk}'}$, $\Phi_{\lambda\lambda'\lambda''}^{\mathbf{kk'k''}}$, etc. could be calculated from frozen-phonon calculations. Compared with the calculation of the harmonic terms, the calculation of the anharmonic terms will have to be more systematic, in order to determine the larger number of anharmonic couplings, and more precise, in order to determine the higher derivatives of the energy surface reliably. As is the case with all frozen-phonon calculations in

a supercell geometry, the couplings can really only be determined at k points which are simple rational fractions of reciprocal lattice vectors. However, the couplings are generally smooth functions of $\mathbf{k}$, at least for nonmetals, and it is possible that some kind of interpolation scheme could be used to approximate the couplings throughout the Brillouin zone. Second, the information obtained in this way could be used as input to a many-body theory, which in turn could be used to calculate a wide variety of physical quantities of interest. These include temperature-dependent phonon self-energies and lifetimes, thermal conductivity, lattice thermal expansion, and phonon-phonon scattering cross sections.

Our goal here is more modest than the ambitious systematic treatment suggested above. Instead, we will illustrate the ideas by calculating an interesting subset of the couplings, namely, those of the optical phonons at the Brillouin zone center. We will also illustrate how these can be used as input to a perturbative many-phonon calculation by calculating the screened two-phonon scattering amplitude, and an estimate of the optical phonon self-energy shift, at zero temperature.

Specializing to the zone center, we consider displacements

$$x_i^{\mathrm{m}} = x_{\tau\lambda}^{\mathrm{m}} = (-1)^{\tau} u_\lambda \tag{12}$$

where the composite index i has been broken into site ($\tau = 1, 2$) and Cartesian ($\lambda = x, y, z$) indices. The normal mode coordinates corresponding to (12) are

$$a_{\mathbf{k}\lambda} = \begin{cases} \sqrt{2N}\, u_\lambda, & \mathbf{k}=0 \\ 0, & \text{otherwise.} \end{cases} \tag{13}$$

(For the zone center phonons, it is convenient to use Cartesian displacement directions x, y, z for the polarization index λ.) Then the potential energy of distortion per cell is

$$\Delta E = \frac{2}{2!}\sum_{\lambda} \Phi^{00}_{\lambda\lambda} u_\lambda^2 + \frac{2}{3!}\sum_{\lambda\lambda'\lambda''} \Phi^{000}_{\lambda\lambda'\lambda''} u_\lambda u_{\lambda'} u_{\lambda''} + \frac{2}{4!}\sum_{\lambda\lambda'\lambda''\lambda'''} \Phi^{0000}_{\lambda\lambda'\lambda''\lambda'''} u_\lambda u_{\lambda'} u_{\lambda''} u_{\lambda'''} \ . \tag{14}$$

Symmetry greatly reduces the number of independent couplings Φ that occur at each order in Eq. (14). $\Delta E(\mathbf{u})$ is symmetric under the operations of the full tetrahedral group T_d, i.e., $\Delta E(\mathbf{u}) = \Delta E(\mathscr{R}\cdot\mathbf{u})$ for $\mathscr{R} \in T_d$. Therefore the number of independent couplings c_n at order n is given by the number of times the identical representation appears in the representation of T_d formed by the fully symmetric nth rank tensors. The value of c_n is most easily obtained[16] from the Molien generating function for T_d,

$$M(t) = \sum_{n=0}^{\infty} c_n t^n = \frac{1}{(1-t^2)(1-t^3)(1-t^4)} \ , \tag{15}$$

and the corresponding invariants can be inferred from the expression of $\Delta E(\mathbf{u})$ in terms of the elementary invariants

$$\Delta E(\mathbf{u}) = f(\theta_1, \theta_2, \theta_3) \tag{16}$$

where

$$\begin{aligned} \theta_1 &= u_x^2 + u_y^2 + u_z^2 \ , \\ \theta_2 &= u_x u_y u_z \ , \\ \theta_3 &= u_x^4 + u_y^4 + u_z^4 \ . \end{aligned} \tag{17}$$

That is, any nth order invariant must be a simple polynomial in the elementary invariants θ_1, θ_2, and θ_3. The only invariants at order 2 and 3 are θ_1 and θ_2, respectively, while two invariants θ_3 and θ_1^2 occur at order 4. Thus we can expand $\Delta E(\mathbf{u})$ to fourth order as

$$\Delta E = \kappa\theta_1 + 6\gamma\theta_2 + \alpha\theta_3 + 3\beta(\theta_1^2 - \theta_3) \ , \tag{18}$$

where

$$\begin{aligned} \kappa &= \frac{2}{2!}\Phi^{00}_{xx} \ , \\ \gamma &= \frac{2}{3!}\Phi^{000}_{xyz} \ , \\ \alpha &= \frac{2}{4!}\Phi^{0000}_{xxxx} \ , \\ \beta &= \frac{2}{4!}\Phi^{0000}_{xxyy} \ . \end{aligned} \tag{19}$$

These four constants are the only independent couplings that occur through fourth order, and our task is reduced to determining these.

The second-order coupling κ is just the spring constant, related to the zone-center frequency by

$$\omega_0 = \sqrt{\kappa/M} \ . \tag{20}$$

The third-order coupling has been discussed by Keating[10] (K), Wendel and Martin[1] (WM), Harmon, Weber and Hamann[5] (HWH), and Yin and Cohen[2] (YC). These authors introduce parameters γ^{K}, k_{xyz}^{WM}, k_{xyz}^{HWH}, and k_{xyz}^{YC}, respectively, which are related to our γ by

$$\gamma = \frac{64}{3}\gamma^{\mathrm{K}} = \frac{2}{\sqrt{3}}k_{xyz}^{\mathrm{WM}} = \frac{4}{3}k_{xyz}^{\mathrm{HWH}} = \frac{4}{3}k_{xyz}^{\mathrm{YC}} \ . \tag{21}$$

The values of γ reported by these authors for Si (Refs. 1, 2, 5, and 10) and Ge (Refs. 2 and 10) will be compared with our results in the next section. The fourth-order constants have not previously been reported in the literature, to our knowledge.

In terms of our parameters, it is easy to verify from Eq. (18) that for displacements in the [100], [110], and [111] directions, respectively, the energy is, to fourth order,

$$\begin{aligned} \Delta E_{[100]} &= \kappa u^2 + \alpha u^4 \ , \\ \Delta E_{[110]} &= \kappa u^2 + (\tfrac{1}{2}\alpha + \tfrac{3}{2}\beta)u^4 \ , \\ \Delta E_{[111]} &= \kappa u^2 + \frac{2\gamma}{\sqrt{3}}u^3 + (\tfrac{1}{3}\alpha + 2\beta)u^4 \ . \end{aligned} \tag{22}$$

The frozen-phonon calculations are carried out by making a series of displacements along these symmetry directions; the four parameters are then obtained by fitting the results to these expressions, as described in the next section.

TABLE I. Convergence tests of plane-wave-basis cutoff for Si.

E_{cut} (Ry)	E_{coh} (eV)	κ (eV Å^{-2})	α (eV Å^{-4})
5	2.70	24.84	−31.90
7	3.56	23.92	−32.39
10	4.40	26.53	−44.81
14	4.74	27.17	−52.14
20	4.81	26.38	−46.76

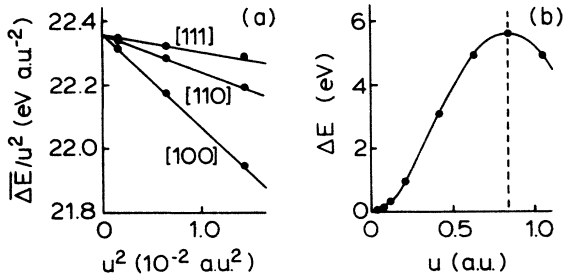

FIG. 1. Energy of distortion ΔE vs displacement u for optical frozen phonon at Brillouin zone center in diamond. (a) Even part of energy change, $\overline{\Delta E}$, plotted on rescaled axes (see text) for small displacements in several directions. (b) Energy change ΔE for large displacements u along the [100] direction. Dots represent the calculated points; the energy curve is symmetric about the dashed line.

III. CALCULATIONS

A. Method

For carbon, a localized-orbital approach, described previously,[6,7] was used. Three decay constants were utilized for each s- or p-type Gaussian orbital in the basis. A Hamann-Schlüter-Chiang (HSC) pseudopotential[17] was used in conjunction with Hedin-Lundqvist exchange-correlation.[18] The G-space total energy sums were carried out to a cutoff of 8 a.u.$^{-1}$. For each displacement direction of the atoms ([100], [110], or [111]), a k-point set was chosen which would map back to the 10-point special k-point set[19] of the undistorted diamond crystal.

For Si and Ge, the calculations were done in a plane-wave basis.[8] A modified version[20] of the HSC scheme was used to generate the pseudopotentials. Wigner exchange-correlation[21] was employed here. The k-point sets were chosen to map back to the 2-point set[19] of the diamond crystal, after tests which indicated that the results were virtually identical to those of the 10-point set used for C. Table I shows the results of tests of the convergence with respect to plane-wave cutoff for Si. The results for the phonon frequency, given by κ, are consistent with those reported previously by Yin and Cohen.[2] The higher order anharmonic couplings, such as α, were found to require a higher level of convergence than the harmonic constant. A cutoff of 14 Ry was adopted for both Si and Ge. The calculations were iterated until the total energy was converged to $<10^{-5}$ eV. Such a fine level of convergence is needed to determine the higher order derivatives with adequate precision. Lowdin perturbation theory[22] was not used, because in the absence of a variational principle the total energy converges too slowly.

The results tabulated below were based upon a set of displacements of u = 0.00, 0.04, 0.08, and 0.12 a.u. of each atom from its equilibrium position for C, and of 0.00, 0.04, 0.08, and 0.12 Å for Si and Ge. (Scaled to the lattice constant, these are all similar.) The displacements were either in the [100], [110], or [111] directions. For a given direction, the terms of the Taylor expansion of $\Delta E(u)$ up to fourth order are determined from a fit of the data points. That this can be done reliably is illustrated for the even derivatives in Fig. 1(a). To eliminate the odd term in $\Delta E_{[111]}$, we define $\overline{\Delta E} \equiv [\Delta E(u)+\Delta E(-u)]/2$. Then we plot $\overline{\Delta E}/u^2$ vs u^2. The intercept at $u^2=0$ gives the second derivative, and the slope gives the fourth derivative. As can be seen from Eq. (22), only one direction is sufficient in principle to determine κ, and any two directions are sufficient to determine α and β. The results for all three directions are shown in Fig. 1(a), where it can be seen that all the intercepts coincide. Moreover, the values of α and β determined from any two of the three slopes are in close agreement. This has been checked for both the localized-orbital and plane-wave calculations. The fact that the curves are nearly linear in Fig. 1(a) indicates that sixth-order terms are not yet important, although they were included in the fit. The results given below were obtained primarily from displacements along [100] and [111] alone; the latter are used to determine the odd term γ, as well as helping to determine α and β.

B. Results and discussion

The central results are given in Table II. In addition to the couplings κ, γ, α, and β, we give the values for the renormalized couplings β' and β'' defined in Sec. IV. The values of the spring constant κ are in close agreement with those given previously.[2,6] The bare phonon frequencies calculated from Eq. (20) are already within $\sim 1\%$ of the experimental frequencies, as can be seen in Table III.

The sign of the third-order coupling γ indicates that it

TABLE II. Calculated coupling constants for optical phonons at Brillouin zone center.

Element	κ (eV Å^{-2})	γ (eV Å^{-3})	α (eV Å^{-4})	β (eV Å^{-4})	β' (eV Å^{-4})	β'' (eV Å^{-4})
C	79.85	−165.2	−370	27	−144	−486
Si	27.17	−48.4	−52	17	−26	−112
Ge	24.34	−39.9	−42	13	−19	−85

TABLE III. Phonon frequencies of optical modes at Γ. $\Delta\omega$ is the self-energy shift; ω_0 and ω_{theor} are the bare and renormalized theoretical values respectively. ω_{expt} is the experimental frequency.

Element	ω_0 (cm^{-1})	$\Delta\omega$ (cm^{-1})	ω_{theor} (cm^{-1})	ω_{expt} (cm^{-1})
C	1344	−17.3	1327	1332
Si	513	−3.5	509	518
Ge	302	−1.2	301	304

is harder to compress the [111] bond than to stretch it. For Si, previous values of −60.6, −46.4, and −43.7 eV Å^{-3} were obtained from frozen-phonon calculations by WM,[1] HWH,[5] and YC,[2] respectively. YC (Ref. 2) obtained a value of −36.9 eV Å^{-3} for Ge. The present results are expected to be the most accurate, given the high degree of convergence used. To our knowledge, the couplings γ have never been measured experimentally. Within the Keating model,[10] γ is directly related to the third-order elastic constants c_{112} and c_{123} by

$$\gamma^K=\frac{3c_{112}+c_{123}}{4}\ . \tag{23}$$

The measured values[23] of c_{112} and c_{123} give $\gamma=-47.1$ and −39.4 eV Å^{-3} for Si and Ge, respectively. In Ref. 10, γ^K is fitted to other data as well; then $\gamma=-46.7$ and −36.2 eV Å^{-3} for Si and Ge, respectively. The agreement with the *ab initio* frozen-phonon calculations is surprisingly good.

To our knowledge, no experimental or theoretical reports of the fourth-order constants α and β have previously appeared for any tetrahedral material. Perhaps the most surprising feature of the results presented here is that the coupling α is strongly negative. This means that as the atoms are displaced along the [100] direction, the restoring force is *weaker* than expected from the harmonic approximation. If the atoms were "bumping into" one another, to the extent that the steeply repulsive part of the two-body interaction were coming into play, the restoring force would be expected to be stronger. In fact, for a displacement along [100], the atoms are "missing" one another. A displacement of $u=a/2$ maps the crystal back into itself, and the energy curve is symmetric about the point $u=a/4$ of closest approach between atoms. The energy curve is actually periodic, and is plotted over one-half of its period in Fig. 1(b). The calculated curve has, plausibly, a cosine-like form; we then expect alternating signs ($\kappa>0$, $\alpha<0,\ldots$) for the second, fourth, etc. derivatives. This is what we find.

Several empirical force-field models which attempt to go beyond the harmonic approximation have been proposed.[10,11] However, models of this type contain a bond-stretching term and generally give the wrong sign for α, because they cannot reproduce the periodic nature of $\Delta E(u)$ without introducing unphysical cusps where the bonds are redefined at $u=a/4$. Recently, a model free of this kind of approximation has been proposed[24] for Si; however, it has not been optimized for phonon properties. The optical phonon parameters presented here should prove useful in constraining future attempts at such models.

In order to make comparisons between the results for C, Si, and Ge, it is useful to scale the calculated coupling constants to dimensionless form. We do this using the bond length d and spring constant κ as the references for length and energy. Thus we define

$$\tilde{\gamma}=\gamma d\kappa^{-1},\quad \tilde{\alpha}=\alpha d^2\kappa^{-1}\ , \tag{24}$$

etc. The results are given in dimensionless form in Table IV. The similarity between the couplings of C and those of Si and Ge is remarkable, given the differences in the shape of the phonon dispersion relations. Not so surprisingly, the couplings of Si and Ge are found to be almost identical when presented in this dimensionless form.

IV. RENORMALIZATION BY PHONON SCREENING

The anharmonic couplings calculated in the previous section determine the bare phonon–phonon interaction amplitudes. For example, inserting Eq. (10a) in (6c) we obtain for the two-phonon scattering amplitude

$$\begin{aligned}\langle 3,4\,|\,V_4\,|\,1,2\rangle&=\frac{1}{4!}\frac{\hbar^2}{8NM^2}\sum_{ijkl}\Phi_{ijkl}(\omega_i\omega_j\omega_k\omega_l)^{-1/2}\\&\quad\times\langle 0\,|\,b_3b_4(b_i+b^\dagger_{-i})(b_j+b^\dagger_{-j})(b_k+b^\dagger_{-k})(b_l+b^\dagger_{-l})b^\dagger_1b^\dagger_2\,|\,0\rangle\\&=\frac{\hbar^2}{8NM^2}(\omega_1\omega_2\omega_3\omega_4)^{-1/2}\Phi^{-\mathbf{k}_1,-\mathbf{k}_2,\mathbf{k}_3,\mathbf{k}_4}_{\lambda_1,\lambda_2,\lambda_3,\lambda_4}\ .\end{aligned} \tag{25}$$

TABLE IV. Calculated coupling constants in dimensionless form.

Element	$\tilde{\gamma}$	$\tilde{\alpha}$	$\tilde{\beta}$	$\tilde{\beta}'$	$\tilde{\beta}''$
C	−3.20	−11.1	0.8	−4.3	−14.5
Si	−4.19	−10.6	3.5	−5.3	−22.9
Ge	−4.01	−10.3	3.3	−4.8	−20.8

The contracted notation $|1\rangle = |\mathbf{k}_1,\lambda_1\rangle$ has been introduced. As long as we are only interested in scattering of phonons in the vicinity of the Brillouin zone center, we may set $\mathbf{k}\approx 0$ and $\omega\approx\omega_0$ for all phonons appearing in (25). Then

$$\langle \mathbf{k}_3 x,\mathbf{k}_4 x \mid V_4 \mid \mathbf{k}_1 x,\mathbf{k}_2 x\rangle \approx \frac{\hbar^2}{8NM^2\omega_0^2}\Phi^{0000}_{xxxx}\delta(\mathbf{k}_1+\mathbf{k}_2-\mathbf{k}_3-\mathbf{k}_4)=\frac{3\hbar^2\alpha}{2NM^2\omega_0^2}\delta(\mathbf{k}_1+\mathbf{k}_2-\mathbf{k}_3-\mathbf{k}_4) \tag{26}$$

and

$$\langle \mathbf{k}_3 x,\mathbf{k}_4 y \mid V_4 \mid \mathbf{k}_1 x,\mathbf{k}_2 y\rangle = \langle \mathbf{k}_3 y,\mathbf{k}_4 y \mid V_4 \mid \mathbf{k}_1 x,\mathbf{k}_2 x\rangle \approx \frac{3\hbar^2\beta}{2NM^2\omega_0^2}\delta(\mathbf{k}_1+\mathbf{k}_2-\mathbf{k}_3-\mathbf{k}_4)\ . \tag{27}$$

Alternatively, the scattering may take place via a virtual intermediate state. In particular, a virtual process involving two three-phonon interactions turns out to contribute to the same order as the single four-phonon interaction above. We use perturbation theory to calculate the amplitude for the virtual process

$$\langle 3,4 \mid V_4' \mid 1,2\rangle = \sum_{\Psi_j}\langle 3,4 \mid V_3 \mid \Psi_j\rangle\frac{1}{E_{12}-E_j}\langle \Psi_j \mid V_3 \mid 1,2\rangle\ . \tag{28}$$

Ψ_j can be a 1-, 3-, or 5-phonon state; it must differ from both the initial and final state by the creation or annihilation of three phonons. For example, $\Psi_j = |2,4,5\rangle$ contributes, provided k conservation is satisfied.

We again consider the case where the external k vectors are nearly zero. Then by k conservation, so are any internal k vectors such as $\mathbf{k}_5$. Then

$$E_{12}-E_j \approx \hbar\omega_0(2-n_j)\ , \tag{29}$$

where n_j is the number of phonons in the intermediate state.

The allowed polarization of the intermediate phonon is heavily constrained by the symmetry expressed in Eq. (19). Only three-phonon processes which involve one x-, one y-, and one z-polarized phonon contribute. The contributions for the scattering of two phonons of unlike polarization, i.e., $xy\rightarrow xy$, are shown in Fig. 2. Thus

$$\begin{aligned}\langle \mathbf{k}_3 x,\mathbf{k}_4 y \mid V_4' \mid \mathbf{k}_1 x,\mathbf{k}_2 y\rangle &\approx \frac{1}{\hbar\omega_0}\sum_{\mathbf{k}_5}(-\langle \mathbf{k}_3 x,\mathbf{k}_4 y \mid V_3 \mid \mathbf{k}_2 y,\mathbf{k}_4 y,\mathbf{k}_5 z\rangle\langle \mathbf{k}_2 y,\mathbf{k}_4 y,\mathbf{k}_5 z \mid V_3 \mid \mathbf{k}_1 x,\mathbf{k}_2 y\rangle+\cdots)\\ &\approx \frac{\hbar^2}{16NM^3\omega_0^4}(\Phi^{000}_{xyz})^2(-1-1+1-\tfrac{1}{3})\delta(\mathbf{k}_1+\mathbf{k}_2-\mathbf{k}_3-\mathbf{k}_4)\\ &= \frac{-3\hbar^2\gamma^2}{4NM^3\omega_0^4}\delta(\mathbf{k}_1+\mathbf{k}_2-\mathbf{k}_3-\mathbf{k}_4)\ ,\end{aligned} \tag{30a}$$

where the four terms appearing on the right correspond to Figs. 2(c)–2(f), respectively. Similarly,

$$\begin{aligned}\langle \mathbf{k}_3 y,\mathbf{k}_4 y \mid V_4' \mid \mathbf{k}_1 x,\mathbf{k}_2 x\rangle &\approx \frac{\hbar^2}{16NM^3\omega_0^4}(\Phi^{000}_{xyz})^2(-1-1-1-1)\delta(\mathbf{k}_1+\mathbf{k}_2-\mathbf{k}_3-\mathbf{k}_4)\\ &= \frac{-9\hbar^2\gamma^2}{4NM^3\omega_0^4}\delta(\mathbf{k}_1+\mathbf{k}_2-\mathbf{k}_3-\mathbf{k}_4)\ ,\end{aligned} \tag{30b}$$

following Figs. 3(c)–3(f), for scattering of the type $xx\rightarrow yy$. Thus while the bare interaction amplitudes for $xx\rightarrow yy$ and $xy\rightarrow xy$ are the same, Eq. (27), the screening for these two processes is different. The bare interaction for scattering of type $xx\rightarrow xx$, Eq. (26), is not screened at this order, because the only nonzero three-phonon vertex, xyz, cannot occur.

These results may be summarized by defining renormalized couplings β' and β'' which replace the bare coupling β for screened interactions of type $xy\rightarrow xy$ and $xx\rightarrow yy$ respectively. Comparing Eqs. (27) and (30), and using (20), we find

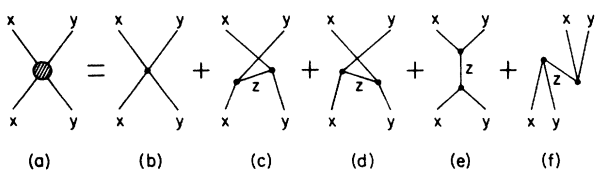

FIG. 2. Diagrammatic representation of screened vertex for scattering of zone-center phonons of unlike polarization, (a), in terms of bare vertex (b) and processes involving virtual phonon exchange, (c)–(f). Labels x,y,z indicate polarization; time runs in the vertical direction.

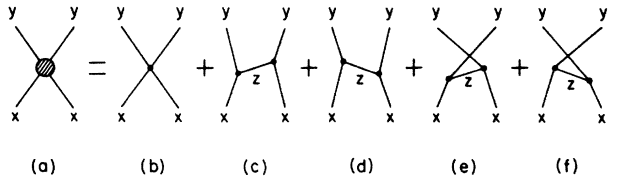

FIG. 3. Diagrammatic representation of screened vertex for scattering of phonons of like polarization, (a), in terms of bare vertex (b) and virtual phonon processes (c)–(f). Labels indicate polarization; time runs in the vertical direction.

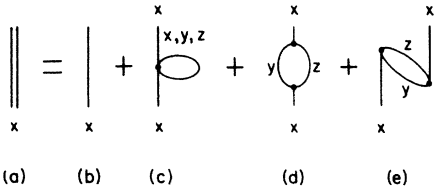

FIG. 4. Diagrammatic representation of renormalized propagator (a) in terms of bare propagator (b) and virtual phonon processes (c)–(e). Labels indicate polarization; time runs in the vertical direction.

$$\beta' = \beta - \gamma^2/2\kappa \,, \tag{31a}$$

$$\beta'' = \beta - 3\gamma^2/2\kappa \,. \tag{31b}$$

The coupling α remains unrenormalized. The values of the renormalized couplings β' and β'' are included in Tables II and IV. It is noteworthy that all three relevant fourth-order couplings α, β', and β'' are negative for all three materials. For diamond, this would appear to rule out[9] the possibility that zone-center optical phonons could form a two-phonon bound state.[12]

We can also attempt to calculate the renormalization of the phonon self-energy. The relevant virtual processes are shown in Fig. 4. Again a single four-phonon process enters at the same order as a pair of three-phonon processes with a virtual intermediate state. The four-phonon contribution is

$$\langle 1 \mid V_4 \mid 1 \rangle = \frac{1}{4!}\frac{\hbar^2}{8NM^2}\sum_{ijkl}\Phi_{ijkl}(\omega_i\omega_j\omega_k\omega_l)^{-1/2}\langle 0 \mid b_1(b_i+b^\dagger_{-i})(b_j+b^\dagger_{-j})(b_k+b^\dagger_{-k})(b_l+b^\dagger_{-l})b^\dagger_1 \mid 0\rangle \,. \tag{32}$$

We only keep terms which do not enter the vacuum expectation energy, since we really want to calculate

$$\hbar\Delta\omega_1^{(4)} \equiv \langle 1 \mid V_4 \mid 1\rangle - \langle 0 \mid V_4 \mid 0\rangle \,. \tag{33}$$

Terms like $b_2 b_2^\dagger b_3 b_3^\dagger$ in V_4 contribute equally to both terms on the right-hand side of (33), and hence do not enter $\Delta\omega_1$. Therefore the terms which do enter are those of the form $b_1 b_1^\dagger b_2 b_2^\dagger$, or any permutation of these in which $b_2^\dagger$ remains to the right of b_2. By (33), the contribution is the same whether $b_1^\dagger$ is to the right or left of b_1, since

$$\begin{aligned}\langle 1 \mid b_1 b_1^\dagger \mid 1\rangle - \langle 0 \mid b_1 b_1^\dagger \mid 0\rangle &= \langle 1 \mid b_1^\dagger b_1 \mid 1\rangle \\ &\quad - \langle 0 \mid b_1^\dagger b_1 \mid 0\rangle \\ &= 1 \,.\end{aligned}$$

So

$$\Delta\omega_1^{(4)} = \frac{\hbar}{16NM^2}\sum_{\mathbf{k}_2\lambda_2}\frac{1}{\omega_1\omega_2}\Phi^{\mathbf{k}_1,-\mathbf{k}_1,\mathbf{k}_2,-\mathbf{k}_2}_{\lambda_1,\lambda_1,\lambda_2,\lambda_2} \,. \tag{34}$$

Now $\mathbf{k}_2$ must be summed over the entire Brillouin zone, even if $\mathbf{k}_1 \approx 0$, so it is no longer appropriate to make the approximation $\Phi \to \Phi^{0000}$. However, in the absence of further information on the k dependence of the fourth-order elastic constants, we make this approximation anyway in order to obtain an order-of-magnitude estimate of the self-energy shift. With this approximation, the N terms in the sum over $\mathbf{k}_2$ contribute equally. For $\lambda_1 = x$, we may have $\lambda_2 = x$, y, or z, and

$$\Delta\omega_1^{(4)} \approx \frac{3\hbar}{4M^2\omega_0^2}(\alpha + 2\beta) \,. \tag{35}$$

This contribution is illustrated in Fig. 4(c).

Finally, we also take into account the virtual contribution of the third-order couplings, Figs. 4(d)–4(e), at the same rough level of approximation:

$$\begin{aligned}\langle \mathbf{k}_1 x \mid V_4' \mid \mathbf{k}_1 x\rangle &\approx -\frac{1}{\hbar\omega_0}\sum_{\substack{\mathbf{k}_2\lambda_2\\ \mathbf{k}_3\lambda_3}} \mid \langle \mathbf{k}_1 x \mid V_3 \mid \mathbf{k}_2\lambda_2, \mathbf{k}_3\lambda_3\rangle \mid^2 - \frac{1}{3\hbar\omega_0}\sum_{\substack{\mathbf{k}_2\lambda_2\\ \mathbf{k}_3\lambda_3}} \mid \langle \mathbf{k}_1 x \mid V_3 \mid \mathbf{k}_1 x, \mathbf{k}_1 x, \mathbf{k}_2\lambda_2, \mathbf{k}_3\lambda_3\rangle \mid^2 \\ &= \frac{-3\hbar\gamma^2}{4M^2\omega_0^2\kappa} \,.\end{aligned} \tag{36}$$

In the sum over $\mathbf{k}_2\lambda_2$ and $\mathbf{k}_3\lambda_3$, there are $2N$ nonzero terms, since a given $\mathbf{k}_2$ fixes $\mathbf{k}_3$ and $(\lambda_2,\lambda_3) = (yz)$ or (zy).

Combining (35) and (36), and using (31a), we find

$$\Delta\omega_1 \approx \frac{3\hbar}{4M^2\omega_0^2}(\alpha + 2\beta') \tag{37}$$

for the estimate of the renormalization of the phonon self-energy by phonon screening. The resulting frequency shifts are given in Table III. The correction to the frequency is on the order of 1%, and becomes relatively less important for the heavier elements. Since the typical errors in local-density calculations of bare phonon frequencies are on the order of 1–2 %, inclusion of the screening

does not significantly improve the agreement with experiment. However, we emphasize that in principle it is the screened frequency, and not the bare frequency that emerges directly from a frozen-phonon calculation, that should be compared with the experimental value.

The analysis given here is strictly applicable only at zero temperature. More sophisticated techniques, such as a Green's function approach, could be applied to obtain information about the temperature dependence of the renormalized couplings and phonon frequencies. However, this would take us beyond the scope of the present work.

V. SUMMARY

We have shown that frozen-phonon calculations can be used to determine bare phonon—phonon scattering amplitudes, and that consideration of virtual processes allows renormalized multiphonon vertices and phonon self-energies to be calculated as well. We have identified and calculated all of the third- and fourth-order coupling constants allowed by symmetry for zone-center optical phonons in the diamond-structure elements C, Si, and Ge, and we have calculated the renormalized couplings where appropriate. The renormalized four-phonon vertices are found to be negative, which appears to rule out the formation of a two-phonon bound state proposed for diamond.

We see no impediment to the application of these techniques to the calculation of anharmonic coupling constants at other points in the Brillouin zone, using supercell geometries. Such information could eventually serve as input to realistic calculations of thermodynamic quantities such as the thermal conductivity, and of phonon self-energy shifts and lifetimes.

ACKNOWLEDGMENTS

Support for the early part of this work, including the calculations on C, was provided by NSF Grant No. DMR83-19024. S.G.L. and D.V. wish to acknowledge support by a program development fund from the Director of the Lawrence Berkeley Laboratory. M.L.C. and S.G.L. acknowledge support by the Director, Office of Energy Research, Office of Basic Energy Sciences, Materials Sciences Division of the U.S. Department of Energy under Contract No. DE-AC03-76SF00098. CRAY computer time was provided by the Office of Energy Research of the Department of Energy. Support for the latter part of this work, including the calculations on Si and Ge, was provided by the NSF through the Harvard Materials Science Laboratory and through Grant No. DMR82-07431; supercomputer time was provided by the NSF Office of Advanced Scientific Computing.

[1]H. Wendel and R. M. Martin, Phys. Rev. Lett. **40**, 950 (1978); Phys. Rev. B **19**, 5251 (1979).
[2]M. T. Yin and M. L. Cohen, Phys. Rev. Lett. **45**, 1004 (1980).
[3]K. Kunc and R. M. Martin, Phys. Rev. Lett. **48**, 406 (1982).
[4]W. Kohn and L. J. Sham, Phys. Rev. **140**, A1133 (1965).
[5]B. N. Harmon, W. Weber, and D. R. Hamann, Phys. Rev. B **25**, 1109 (1982).
[6]J. R. Chelikowsky and S. G. Louie, Phys. Rev. B **29**, 3470 (1984).
[7]D. Vanderbilt and S. G. Louie, Phys. Rev. B **30**, 6118 (1984).
[8]J. Ihm, A. Zunger, and M. L. Cohen, J. Phys. C **12**, 1979.
[9]D. Vanderbilt, S. G. Louie, and M. L. Cohen, Phys. Rev. Lett. **53**, 1477 (1984).
[10]P. N. Keating, Phys. Rev. **149**, 674 (1966).
[11]S. L. Altmann, A. Lapiccirella, K. W. Lodge, and N. Tomassini, J. Phys. C **15**, 5581 (1982); S. L. Altmann, K. W. Lodge and A. Lapiccirella, Philos. Mag. A **47**, 827 (1983).
[12]M. H. Cohen and J. Ruvalds, Phys. Rev. Lett. **23**, 1378 (1969); see also J. Ruvalds and A. Zawadowski, Phys. Rev. B **2**, 1172 (1970).
[13]S. A. Solin and A. K. Ramdas, Phys. Rev. B **1**, 1687 (1970).
[14]R. Tubino and J. L. Birman, Phys. Rev. Lett. **35**, 670 (1975); Phys. Rev. B **15**, 5843 (1977).
[15]G. Leibfried and W. Ludwig, Solid State Phys. **12**, 276 (1961).
[16]M. V. Jarić, L. Michel and R. T. Sharp, J. Phys. (Paris) **45**, 1 (1984), and references therein.
[17]D. R. Hamann, M. Schlüter, and C. Chiang, Phys. Rev. Lett. **43**, 1494 (1979).
[18]L. Hedin and B. I. Lundqvist, J. Phys. C **4**, 2064 (1971).
[19]D. J. Chadi and M. L. Cohen, Phys. Rev. B **8**, 5747 (1973).
[20]D. Vanderbilt, Phys. Rev. B **32**, 8412 (1985).
[21]E. P. Wigner, Phys. Rev. **36**, 1002 (1934).
[22]P. Lowdin, J. Chem. Phys. **19**, 1396 (1951).
[23]H. J. McSkimin and P. Andreatch, Jr., J. Appl. Phys. **35**, 3312 (1965).
[24]R. Biswas and D. R. Hamann, Phys. Rev. Lett. **55**, 2001 (1985).